Solidification of ^{4}He confined in a nanometer-size channel

Junko Taniguchi* and Masaru Suzuki
Department of Engineering Science, University of Electro-Communications, Chofu, Tokyo 182-8585, Japan
(Received 25 March 2011; revised manuscript received 14 May 2011; published 5 August 2011)

Solidification of ^{4}He confined in a one-dimensional 2.8-nm channel of FSM was studied by pressure and heat capacity measurements. It was found that the freezing pressure in the channel is greatly elevated and is between 3.3 and 3.8 MPa at absolute zero. Furthermore, the density change at the liquid-solid transition is evaluated. The decrease in the molar volume is less than 1×10^{-2} cm^3/mol at the transition of 4 MPa, which is about two orders of magnitude smaller than that of bulk. From this observation, we can conclude that solid ^{4}He confined in the channel has a density as low as liquid.

DOI: 10.1103/PhysRevB.84.054511 PACS number(s): 67.80.B−, 67.80.de, 61.46.−w

I. INTRODUCTION

Solidification of liquids confined in a porous medium has attracted the attention of researchers over the years.[1,2] In various porous media, the elevation of freezing pressure or the depression of freezing temperature were commonly observed.[3,4] This elevation and depression are closely related to the mechanism for the nucleation of solid in the pores, and can be explained by the homogeneous nucleation theory. However, when the pore size becomes much smaller, it is expected that the freezing cannot be explained by the homogeneous nucleation theory using the properties of bulk solid. In addition, the confinement changes the behavior of transition between liquid and solid. The molecular dynamics simulation has revealed that freezing of water inside carbon nanotubes occurs continuously; in contrast to the first order transition between bulk liquid and solid, there is no intrinsic distinction between the two phases confined in a one-dimensional (1D) nanometer-size channel.[5] In fact, by x-ray diffraction measurements, it was found that CH_3OH vitrifies on freezing inside a 1D nanometer-size channel,[6] and the glass transition of cyclohexane and benzene confined in the channel was observed by differential scanning calorimetry and NMR.[7]

Furthermore, since the observation in torsional oscillator measurements by Kim and Chan[8] of a nonclassical rotational inertia (NCRI) on solid ^{4}He confined in a nanoporous glass, Vycor, a great interest has focused on the quantum behavior of solid ^{4}He. Those researchers have reported that solid ^{4}He confined in Vycor shows the supersolid fraction of 0.5% at low temperatures. Although the NCRI was also observed for bulk solid ^{4}He, the supersolid fraction varied over the range 0.01%–20% in various experiments.[9–11] In addition, glassy behavior is observed near the onset of NCRI.[12–14] This may suggest that the NCRI depends on the property of noncrystalline solid rather than pure single-crystalline solid.

By analogy with classical liquids, the confinement is expected to change the properties of ^{4}He. Very recently, neutron-scattering measurements have shown that ^{4}He confined in a 4.7-nm channel experiences a transition from liquid to amorphous solid.[15] Thus, we have performed freezing pressure and heat capacity measurements on ^{4}He confined in a 1D uniform nanometer-size channel of folded sheets mesoporous materials (FSM) with a 2.8-nm channel. In this paper, we present a phase diagram of solid-liquid transition in the channel, and the properties of solid ^{4}He.

II. EXPERIMENT

The porous medium FSM we used was synthesized by Inagaki *et al.* at Toyota Central R&D Labs., Inc. Japan.[16] It forms a honeycomb structure of a 1D uniform nanometer-size straight channel without interconnection. In the present work, we used an FSM sample whose channel diameter was 2.8 nm from the same batch used in the previous work on the superfluidity of liquid ^{4}He by torsional oscillator measurements.[17]

The FSM sample was powder of 0.2–0.5 μm in size, which was formed into a pellet as follows: first, the FSM powder was heated at 120 °C for 8 h to allow it to dehydrate. Then the FSM and 70 μm silver powders were mixed in a two-to-one mass ratio. The mixed powder was pressed in metal jigs under 700 kgf/cm^2, resulting in a pellet of ϕ10.0 mm × t4.5 mm. A pellet was then sintered at 200 °C for 3 h. From Brunauer-Emmett-Teller (BET) fitting to the N_2 adsorption isotherm, the surface area of the pellet was obtained as 182 m^2, and volume of the 2.8-nm channel was estimated to be 138 mm^3 from the surface-volume ratio of FSM powder.[18]

The sample cell shown in Fig. 1 was used for both freezing pressure and heat capacity measurements. The height including the pressure gauge is about 14 mm. The pellet was put into a BeCu container ϕ13.0 mm × t7.7 mm, whose top side wall acted as a diaphragm of the Straty-Adams-type capacitive pressure gauge.[19] In the container, there were open spaces between FSM powders in the pellet, and between the pellet and the container. The total volume of the open spaces was 113 ± 8 mm^3. The cell was attached to a dilution refrigerator, and was thermally linked weakly to an isothermal copper stage via a thin Ag wire and a CuNi capillary of 50 μm ID. As thermometers, RuO_2 and Ge bare chip resistors were glued onto the cell. An RuO_2 thermometer was used for the low temperature region below 1.6 K, while a Ge one for the high temperature region. They were calibrated against an RuO_2 thermometer calibrated by Lake Shore Cryotronics Inc. A strain gauge with a resistance of 120 Ω was also attached on the cell as a heater. The lowest temperature of the cell was 0.2–0.4 K, depending on pressure.

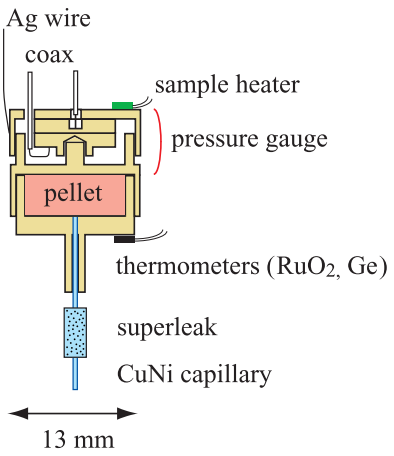

FIG. 1. (Color online) Schematic view of the sample cell.

We prepared solid ^{4}He by a blocked capillary method. Liquid ^{4}He was introduced via a CuNi capillary of 5 m $\times$ ID 50 μm. Between the isothermal stage and the cell, a superleak made of Vycor was inserted. This setup inhibited the migration of solid ^{4}He in the capillary, and makes the amount of ^{4}He in the container constant, after ^{4}He in the capillary solidified. To solidify ^{4}He, the cell was pressurized at around 4.2 K, and cooled down slowly. First, ^{4}He in the open space between the pellet and the container began to solidify, followed by the ^{4}He between the FSM powders. Below the temperature where the bulk solidification was completed, the cooling and warming rate was controlled at 0.9–3 mK/min, by the temperature control of the isothermal stage. It was found that the pressure followed temperature change without a time delay.

The pressure was measured by the above-mentioned gauge which was calibrated against a pressure gauge located at room temperature (Setra 204). Its resolution was better than 6×10^{-4} MPa. On the other hand, for heat capacity measurements, a quasiadiabatic heat-pulse method was adopted. The relaxation time from the cell to the isothermal copper stage was 200–4000 s, which was one order of magnitude larger than that inside the cell, 10–100 s. The temperature stability was better than 30 μK for all the temperature region, and the absolute accuracy of the heat capacity was about 8×10^{-4} J/K at 1.5 K.

III. RESULTS

A. Freezing pressure

The pressure measurements were performed in the region between 2.8 and 6.7 MPa at the lowest temperature. During the measurements along the isochore at constant volume, ^{4}He in the channel communicated with bulk ^{4}He around the FSM powder. We show typical behaviors of the pressure along an isochore where ^{4}He in the channel remained liquid, and where it was frozen.

Figure 2(a) shows the pressure variation and the temperature derivative of pressure, dP/dT, for the case where ^{4}He in the channel remained liquid. As the solidification of bulk ^{4}He in the open spaces in the container proceeded, the pressure decreased along the bulk freezing curve. In cooling,

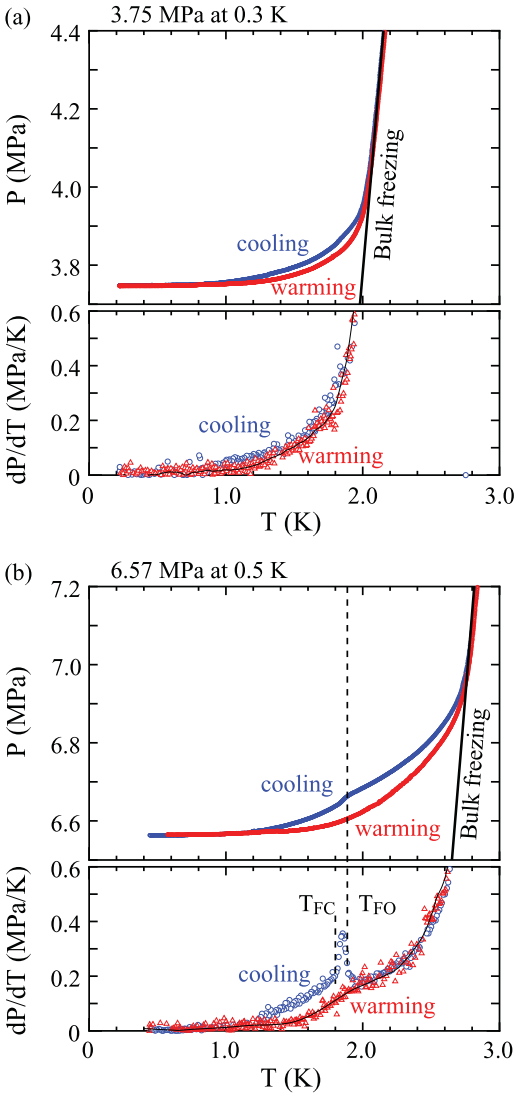

FIG. 2. (Color online) Pressure isochores in warming and cooling and corresponding dP/dT for the sample (a) under 3.75 MPa at 0.3 K, and (b) under 6.57 MPa at 0.5 K. T_{FO} and T_{FC} indicate the temperatures at the freezing onset and completion, respectively.

the pressure smoothly deviated from the bulk freezing curve at around 2.07 K, after the completion of the solidification of bulk ^{4}He. As the temperature was decreased, it decreased gradually down to 3.75 MPa at the lowest temperature mainly because of the thermal contraction of bulk ^{4}He in the open spaces. In warming, the pressure increased smoothly until it reached the bulk freezing curve. A hysteresis between cooling and warming appeared in the temperature region of 0.95–2.07 K, because of the vacancy diffusion in bulk solid ^{4}He.[20] From the pressure variation, dP/dT increased at an accelerated rate at high temperature. It is found that no distinctive feature is observed at this isochore.

Next, we focus on the case where the freezing takes place in the channel. The pressure variation is shown in the upper panel of Fig. 2(b). After the completion of the solidification of bulk ^{4}He, the pressure deviated from the bulk freezing curve at around 2.75 K. In cooling, it decreased gradually

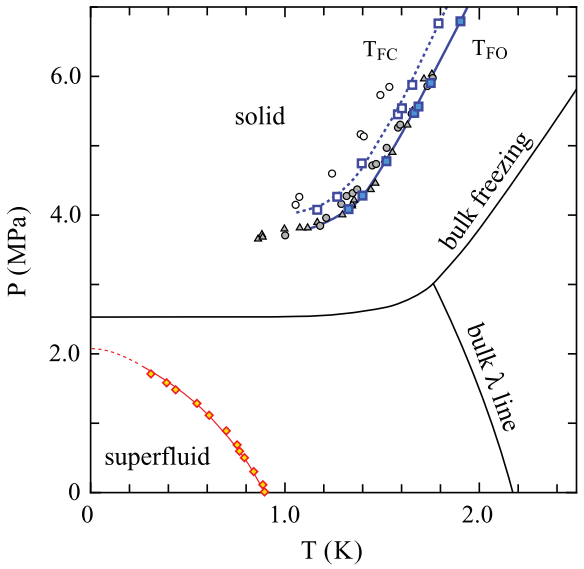

FIG. 3. (Color online) Pressure-temperature phase diagram of the freezing onset and completion. Solid and open symbols indicate T_{FO} and T_{FC}, respectively. Squares: FSM (2.8 nm in the present measurements), circles: Vycor (nominal pore size of 6.0 nm) (Ref. 27), triangles: Gelsil (nominal pore size of 2.5 nm) (Ref. 28). Diamond symbols at low pressure denote the superfluid onset temperature of liquid ^{4}He in the 2.8-nm channel of FSM (Ref. 17).

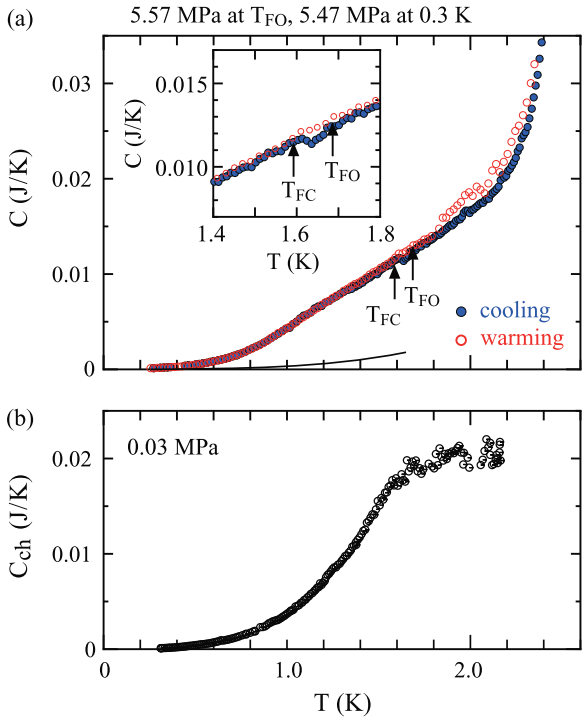

FIG. 4. (Color online) (a) Heat capacity in cooling (solid circles) and in warming (open circles) for the sample which begins to freeze at 5.47 MPa. The solid curve shows the bulk solid ^{4}He contribution. (Inset) Expanded view in the neighborhood of T_{FO} and T_{FC}. (b) Heat capacity of liquid ^{4}He in the channel under 0.03 MPa.

to 6.67 MPa at 1.90 K. With further decreasing temperature, it showed a small drop at around 1.89 K, and returned to a slow decrease at around 1.81 K, then finally approached a constant pressure. This drop was caused by an increase in the density of the channel due to the freezing. As shown in the lower panel of Fig. 2(b), dP/dT in cooling showed a clear peak, during the drop of pressure. We then determined the freezing onset temperature T_{FO} and the freezing completion temperature T_{FC} by the beginning and the end of the peak, respectively.

In warming, the pressure increased smoothly until it reached the bulk freezing curve. Between cooling and warming, there appeared a hysteresis in the temperature region of about 1.2–2.75 K. In contrast to cooling, the pressure change due to the melting was not clearly observed. On the other hand, dP/dT increased at around 1.55 K and its slope changed weakly at around 2.05 K, although it had no peak. This behavior may be attributed to the density change in the channel due to the melting. If we adopt a temperature of 2.05 K as the melting completion, it was slightly higher than T_{FC} of 1.90 K, which means that a weak supercooling took place. The weak change in dP/dT made it difficult to determine the melting onset and completion temperatures precisely.

T_{FO} and T_{FC} are plotted in the phase diagram shown in Fig. 3. For the five isochores between 2.80 and 3.87 MPa, the peak of dP/dT was not detected at the lowest temperature within experimental precision. It was found that the freezing temperature in the channel of FSM was greatly depressed; the freezing onset curve shifts to a lower temperature by 0.84 K at 5.0 MPa, compared with the bulk one. In addition, up to at least 3.27 MPa, ^{4}He in the channel seemed to remain liquid at low temperature, which is discussed later.

B. Heat capacity

We measured the heat capacity simultaneously with the pressure measurements for several isochores to investigate the freezing of ^{4}He confined in the channel. Figure 4(a) shows typical data which experience a transition from liquid to solid in the channel. In the figure, the bulk solid ^{4}He contribution of the open spaces was not subtracted, since its contribution was small. For comparison, the heat capacity of liquid ^{4}He at 0.03 MPa is shown in Fig. 4(b). The data were obtained by subtracting the heat capacity of bulk liquid ^{4}He.

Regarding Fig. 4(a), it was first found that the heat capacity of ^{4}He confined in the channel was obviously larger than that of the open spaces, although the volume of the channel was almost the same as that of the open spaces. This capacity increased gradually at low temperature, and its increase changed to a linear T-dependence around 1 K. With reaching the bulk freezing curve, it showed a rapid increase due to the melting of bulk ^{4}He in the open spaces. In addition, it was also found that no large peak exists in cooling between T_{FO} and T_{FC}. And in warming, no peak was neither observed in the temperature region of about 1.43–1.92 K, where dP/dT shows a rapid increase as mentioned in Sec. III A. The heat capacity in warming was slightly larger than that of cooling between T_{FO} and T_{FC}. This suggests that the difference results from the latent heat in warming around this temperature, and the amount of this heat is small.

We also found that the heat capacity becomes slightly larger than that in cooling at around 1.9 K and this remains until

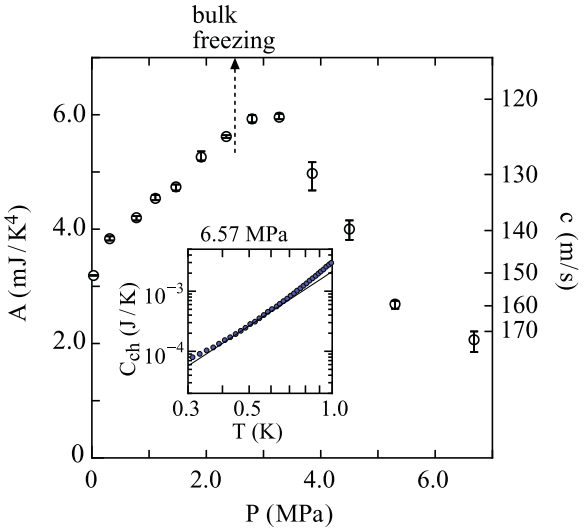

FIG. 5. (Color online) Fitting parameter A as a function of pressure. Arrow points to the freezing pressure of bulk ^{4}He. The freezing in the channel takes place between 3.27 and 3.80 MPa at low temperature. (Inset) Log-log plot of the heat capacity under 6.68 MPa. Solid line is the T^3-term of $C_{\rm ch} = AT^3 + BT$. Below about 0.4 K, the heat capacity deviates from this term due to the T-term. The right vertical axis shows the corresponding sound velocity.

reaching the bulk freezing curve. Although it was difficult to measure the heat capacity precisely at high temperature, this may be partly related to the pressure difference between cooling and warming.[21]

On the other hand, the heat capacity in Fig. 4(b) increased rapidly around 1 K, and showed a broad bump at around 1.6 K. At this pressure, the superfluidity of liquid ^{4}He in the channel was observed, and this behavior is discussed in relation with BEC in the channel.[22]

Comparing between the two sets of data, we found that the heat capacity of Fig. 4(a) is characteristic of a slower increase up to 1 K and the linear T-dependence above 1 K. Furthermore, it was noticed that the heat capacity at low temperature helps to decide whether ^{4}He confined in the channel is solid or not. This capacity between 0.3 and 0.7 K is roughly proportional to T^3, and it can be well fitted below 0.7 K as $C_{\rm ch} = AT^3 + BT$, where $C_{\rm ch}$ is the heat capacity, and A and B are the fitting parameters, as shown in the inset of Fig. 5.[23] Figure 5 shows the fitting parameter A as a function of pressure. A increases almost linearly below 2.80 MPa with increasing pressure, and takes a maximum value around 3.27 MPa. With further increase in pressure, it decreases rapidly. This behavior demonstrates that the property of ^{4}He confined in the channel is changed between 3.27 and 3.80 MPa. From pressure measurements, the freezing is clearly observed above 4.09 MPa. Thus, we can conclude that the freezing pressure in the channel is between 3.27 and 3.80 MPa at low temperature. Here, it is remarked that A does not show a large discontinuity at the freezing pressure.

At present, we do not fully understand the origin of the T^3-dependence. It is well known that the T^3-dependence of the heat capacity can be explained by the three-dimensional (3D) phonon, and the sound velocity c is evaluated by the Debye model as

$$c = \left(\frac{2\pi^2 k_B^4}{15\hbar^3} \frac{V}{A} \right)^{1/3}. \quad (1)$$

Here, V is the volume of FSM powder in the pellet as 268 mm^3, i.e., the honeycomb structure and its channel.[24] This means that the contribution to $C_{\rm ch}$ is thought to be from the honeycomb structure and ^{4}He atoms in the channel. With increasing pressure, c decreases from 150 to 120 m/s below 2.80 MPa, and takes the minimum value around 3.27 MPa. It then increases rapidly and becomes 170 m/s at 6.68 MPa. It is reasonable that the hardening takes place at the liquid-solid transition between 3.27 and 3.80 MPa.

Finally, we make a comment on the 3D phonon in this system. The typical wavelength of thermally excited phonons, λ, is expressed as $\lambda = hc/k_{\rm B}T_{\rm e}$, and becomes larger with decreasing temperature. By using c =150 m/s, we can evaluate λ = 14 nm at 0.5 K. This value is larger than the lattice constant of the honeycomb structure of FSM, and suggests that the phonons are transmitted through the silicate layers of FSM.

C. Molar volume change at the freezing

We evaluated the molar volume change of ^{4}He in the channel at the freezing by two approaches: one is the pressure drop at the freezing, and the other is the latent heat with the Clausius-Clapeyron law. The calculated values by the two different approaches are almost the same, and we found this change to be significantly small.

First, we explain the evaluation from the pressure drop at the freezing. Along the isochore at constant volume, ^{4}He in the channel communicates with bulk ^{4}He in the open spaces around the FSM powder. After completion of the freezing in the open spaces, the change in molar volume is thought to be negligible until it reached the freezing onset in the channel. Because of the conservation of mass between the two coupled volumes, the molar volume change in the channel $\Delta v_{\rm ch} \equiv v_{\rm ch}({\rm liquid}) - v_{\rm ch}({\rm solid})$ is related to the pressure drop ΔP at the freezing as follows:

$$\frac{\Delta v_{\rm ch}}{v_{\rm ch}} = \left(\frac{V_{\rm bulk}}{V_{\rm ch}} \right) \left(\frac{v_{\rm ch}}{v_{\rm bulk}} \right) K \Delta P, \quad (2)$$

where $V_{\rm bulk}/V_{\rm ch}$ is the volume ratio between the open spaces and the *effective* channel, $v_{\rm bulk}$ and $v_{\rm ch}$ are the molar volumes, and K is the bulk compressibility. Here, the molar volume ratio is calculated from the pressure drop at the freezing of bulk ^{4}He in the open spaces on the assumption that the adsorbed inert layer in the channel is unchanged. Since the adsorbed inert layer is about 0.6 nm in thickness,[25] the volume of the *effective* channel is estimated to be $V_{\rm ch}$ = 45 mm^3 and the volume ratio $V_{\rm bulk}/V_{\rm ch}$ = 2.5. Here, ΔP is obtained as the difference between the extrapolations of the time variation before and after the freezing, as shown in Fig. 6(a).

We also evaluate the molar volume change from the latent heat using the Clausius-Clapeyron law. The molar latent heat of the freezing is obtained from the heat current

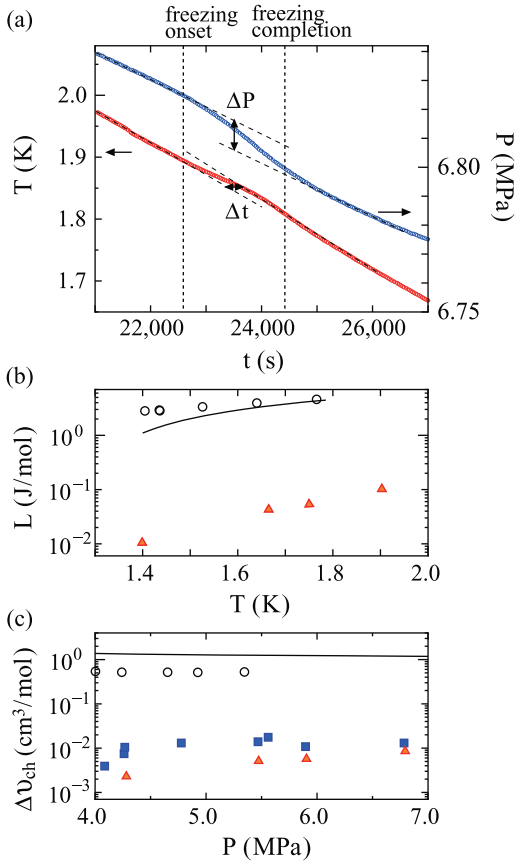

FIG. 6. (Color online) (a) Temperature and pressure in cooling as a function of time. (b) Molar latent heat of the freezing in the channel as a function of temperature. (c) Molar volume change in the channel at the freezing as a function of pressure. Squares and triangles show the data obtained from the drop of pressure and the latent heat, respectively. For comparison, circles in (b) and (c) are the data of Vycor (Ref. 32), and solid curves are the data of bulk ^{4}He.

$\dot{Q} = \Lambda(T_{\rm cell} - T_{\rm st})$ and the additional time Δt at the freezing during a constant cooling rate as

$$L = \frac{\dot{Q}}{n}\Delta t, \tag{3}$$

where n is the molar number of ^{4}He, Λ and $T_{\rm cell} - T_{\rm st}$ are the thermal conductivity and the temperature difference between the cell and the isothermal copper stage.[26] Δt is obtained from the difference between the extrapolations of the temperature variation before and after the freezing, as shown in Fig. 6(a). The molar latent heat of the freezing is shown as a function of pressure in Fig. 6(b). From this value, the molar volume change is calculated as

$$\Delta v_{\rm ch} = \frac{L}{T}\frac{1}{(dP/dT)_{\rm fr}}, \tag{4}$$

where $(dP/dT)_{\rm fr}$ is the slope of the freezing onset curve in Fig. 4.

$\Delta v_{\rm ch}$ obtained by the two approaches is summarized as a function of pressure in Fig. 6(c), and approximately agrees. The decrease in the molar volume at the freezing is less than 0.3%, and is two orders of magnitude smaller than that of bulk ^{4}He. Thus, we can conclude that the density of solid ^{4}He confined in the 2.8-nm channel is as low as liquid.

IV. DISCUSSION

We found that the freezing pressure of ^{4}He confined in the 2.8-nm channel is elevated and is between 3.27 and 3.80 MPa at low temperature. In addition, the decrease in the molar volume of ^{4}He at the freezing was found to be two orders of magnitude less than that of bulk ^{4}He.

First, we compare the elevation of freezing pressure in two nanoporous glasses, Vycor (nominal pore size of 6.0 nm)[27] and Gelsil (2.5 nm).[28] The freezing pressure for these glasses is plotted in Fig. 3, associated with the present work. For Vycor, the decrease in molar volume and the molar latent heat are also plotted in Fig. 6. It is worth notice that the elevation of freezing pressure does not depend strongly on nanoporous media. By application of the homogeneous nucleation theory, the elevation of freezing pressure ΔP_F is calculated as

$$\Delta P_F = \frac{2\alpha_{LS}}{R}\frac{v_{\rm ch}}{\Delta v_{\rm ch}}, \tag{5}$$

where R is the typical pore radius, and α_{LS} is the interfacial tension between liquid and solid.

When α_{LS} and $\Delta v_{\rm ch}$ do not depend on pore radius, ΔP_F is in inverse proportion to R, which does not agree with experimental observations. However, this discrepancy can be resolved. In a naive model, the interfacial tension α is related to the molar volume difference as $\alpha \propto D(\Delta v)^2/\chi v^2$, where D is the interfacial thickness and χ is the isothermal compressibility.[29] If we adopt this model for the interfacial tension of ^{4}He in the channel, $\Delta P_F \propto D\Delta v_{\rm ch}/\chi R v_{\rm ch}$. This suggests that the decrease in molar volume difference between liquid and solid causes a suppression of the elevation of the freezing pressure.

Next, we make a comment on solid ^{4}He in the 2.8-nm channel. Very recently, neutron scattering measurements were carried out for ^{4}He confined in 1D 4.7-nm channel MCM41 and Gelsil (nominal pore size of 3.4 nm).[15] It was reported that the Bragg peak in the static structure factor due to the crystalline of solid is not observed for solid ^{4}He in MCM41, and it is not crystalline but amorphous. Furthermore, it is also suggested that its density is close to liquid ^{4}He in MCM41.

Both from the fact that the molar volume change for the 2.8-nm channel is significantly small and from the neutron scattering measurements, it is thought that solid ^{4}He confined in this channel is amorphous. This may be supported by the heat capacity measurements. In the present work, it was found the specific heat of solid ^{4}He confined in the 2.8-nm channel is obviously large around 1 K compared with that of bulk solid ^{4}He, and shows a linear T-dependence. This can be attributed to the two-level system due to a glasslike state. Here, it is of interest to compare *bulk liquid* ^{4}He. It is well known that the specific heat of bulk liquid ^{4}He also shows a glasslike behavior.[30] It has the linear T-dependence between around 2 and 9 K, and this coefficient at 2.5 MPa is about 2.1 J/K^2 mol. On the other hand, the coefficient of the linear T-dependence for solid ^{4}He in a 2.8-nm channel ranges from 4 to 5 J/K^2 mol. It is worth noting that these values are of similar magnitude to *bulk liquid* ^{4}He.

Finally, we note the difference in the molar latent heat at the freezing between the 2.8-nm channel of FSM and other porous media. It was reported that the molar latent heat at the freezing for Vycor (6.0 nm) is as large as that of bulk ^{4}He.[32] In addition, in the specific heat measurements of Gelsil (2.5 nm), a clear peak at the melting due to the latent heat was also observed.[31] Since the pore size is smaller than the neutron scattering measurements,[15] ^{4}He, at least when confined in Gelsil (2.5 nm) is expected to be amorphous. From the difference in the molar latent heat between the present work and Gelsil, it seems most probable that the amorphous state of ^{4}He in a 1D nanometer-size channel is different from that of porous media with a 3D network. This is left for future study.

V. SUMMARY

Solidification of ^{4}He confined in the 2.8-nm channel of FSM was studied by pressure and heat capacity measurements. The freezing pressure in the channel is greatly elevated to between 3.3 and 3.8 MPa at absolute zero. We also evaluated the molar volume change at the freezing by two approaches: by the pressure drop at the freezing, and by the latent heat using the Clausius-Clapeyron law. The obtained change was more than two orders of magnitude smaller than that of bulk ^{4}He, and solid ^{4}He confined in the 2.8-nm channel had a density as low as liquid, which indicates that solid ^{4}He is amorphous. This is also supported by the T-linear heat capacity around 1 K, which is characteristic of glass.

ACKNOWLEDGMENTS

This work was supported by a Grant-in-Aid for Scientific Research on Priority Areas, "Physics of Super-clean Materials" from the Ministry of Education, Culture, Sports, Science and Technology, Japan.

*tany@phys.uec.ac.jp

[1] L. D. Geib, K. E. Gubbins, R. Radhakrishnan, and M. Sliwinska-Bartkowiak, Rep. Prog. Phys. **62**, 1573 (1999).
[2] E. Molz, A. P. Y. Wong, M. H. W. Chan, and J. R. Beamish, Phys. Rev. B **48**, 5741 (1993) and references therein.[4–20]
[3] E. D. Adams, K. Uhlig, Y.-H. Tang, and G. E. Haas, Phys. Rev. Lett. **52**, 2249 (1984).
[4] J. R. Beamish, A. Hikata, L. Tell, and C. Elbaum, Phys. Rev. Lett. **50**, 425 (1983).
[5] K. Koga, G. T. Gao, H. Tanaka, and X. C. Zeng, Nature **412**, 802 (2001).
[6] K. Morishige and K. Kawano, J. Chem. Phys. **112**, 11023 (2001).
[7] G. Dosseh, Y. Xia, and C. Alba-Simionesco, J. Phys. Chem. B **107**, 6445 (2003).
[8] E. Kim and M. H. W. Chan, Nature **427**, 225 (2004).
[9] E. Kim and M. H. W. Chan, Science **305**, 1941 (2004).
[10] A. S. C. Rittner and J. D. Reppy, Phys. Rev. Lett. **97**, 165301 (2006); **98**, 175302 (2007).
[11] A. C. Clark, J. T. West, and M. H. W. Chan, Phys. Rev. Lett. **99**, 135302 (2007).
[12] B. Hunt, E. Pratt, V. Gadagkar, M. Yamashita, A. V. Balatsky, and J. C. Davis, Science **324**, 632 (2009).
[13] Y. Aoki, M. C. Keiderling, and H. Kojima, Phys. Rev. Lett. **100**, 215303 (2008).
[14] Z. Nussinov, A. V. Balatsky, M. J. Graf, and S. A. Trugman, Phys. Rev. B **76**, 014530 (2007).
[15] J. Bossy, T. Hansen, and H. R. Glyde, Phys. Rev. B **81**, 184507 (2010).
[16] S. Inagaki, A. Koiwai, N. Suzuki, Y. Fukushima, and K. Kuroda, Bull. Chem. Soc. Jpn. **69**, 1449 (1996); S. Inagaki, Y. Fukushima, and K. Kuroda, J. Chem. Soc. Chem. Commun. **22**, 680 (1993).
[17] J. Taniguchi, Y. Aoki, and M. Suzuki, Phys. Rev. B **82**, 104509 (2010).
[18] Private communication with S. Inagaki. The surface-volume ratio is obtained from the data with a surface area of 1176 m^2/g and a pore volume of 0.991 ml/g.
[19] G. C. Straty and E. D. Adams, Rev. Sci. Instrum. **40**, 1393 (1969).
[20] I. Iwasa, K. Araki, and H. Suzuki, J. Phys. Soc. Jpn. **40**, 1119 (1979).
[21] The heat capacity above around 2 K weakly decreases with increasing pressure.
[22] J. Taniguchi, R. Fujii, and M. Suzuki (unpublished).
[23] Here, C_{ch} is the heat capacity after the bulk ^{4}He contribution in the open spaces was removed even when bulk ^{4}He was solid.
[24] From a private communication with S. Inagaki, the lattice constant of the honeycomb structure of FSM is 3.9 nm. The volume of FSM powder is evaluated as $V \sim 138\ m^2 \times (3.9\ nm/2.8\ nm)^2 = 268\ mm^3$.
[25] J. Taniguchi, Doctoral thesis, Tokyo University, 2004.
[26] The thermal conductivity Λ is obtained from the relaxation time from the cell to the isothermal copper stage for the heat capacity measurements.
[27] E. D. Adams, Y. H. Tang, K. Uhlig, and G. E. Haas, J. Low Temp. Phys. **66**, 85 (1987).
[28] K. Yamamoto, Y. Shibayama, and K. Shirahama, J. Phys. Soc. Jpn. **77**, 013601 (2008).
[29] C. A. Croxton, *Statistical Mechanics of the Liquid Surface* (Wiley Interscience Publication, Australia, 1980).
[30] A. F. Andreev, Pis'ma Zh. Eksp. Teor. Fiz. **28**, 603 (1978) [JETP Lett. **28**, 556 (1978)].
[31] K. Yamamoto, Y. Shibayama, and K. Shirahama, Phys. Rev. Lett. **100**, 195301 (2008).
[32] D. N. Bittner and E. D. Adams, J. Low Temp. Phys. **97**, 519 (1994).